Antiferromagnetism of ternary lanthanide stannides RAuSn (R = Pr, Nd, Gd - Er)

1997 J. Phys.: Condens. Matter 9 9053

(http://iopscience.iop.org/0953-8984/9/42/019)

J. Phys.: Condens. Matter **9** (1997) 9053–9063. Printed in the UK PII: S0953-8984(97)83602-8

Antiferromagnetism of ternary lanthanide stannides RAuSn (R = Pr, Nd, Gd–Er)*

S Baran†, M Hofmann‡, J Leciejewicz§, M Ślaski‖, A Szytuła†+ and A Zygmunt¶

† Institute of Physics, Jagellonian University, Reymonta 4, 30-059 Kraków, Poland
‡ Berlin Neutron Scattering Centre, Hahn–Meitner Institut, Glienicker Strasse 100, D-14109 Berlin, Germany
§ Institute of Nuclear Chemistry and Technology, Dorodna 16, 03-169 Warszawa, Poland
‖ School of Physics and Space Research, University of Birmingham, Edgbaston, Birmingham, B14 2TT, UK
¶ Institute of Low Temperatures and Strucutre Research, Polish Academy of Sciences, 50-950 Wrocław, PO Box 937, Poland

Received 22 April 1997, in final form 8 July 1997

Abstract. Neutron diffraction and magnetometric data show that hexagonal (LiGaGe-type crystal structure) RAuSn compounds (R = Pr, Nd, Gd, Tb, Dy, Ho) order antiferromagnetically at low temperatures. Their magnetic structures are described by the wavevector $\boldsymbol{k} = [\frac{1}{2}, 0, 0]$; the magnetic moments are normal to the hexagonal axis in TbAuSn and DyAuSn, parallel to it in PrAuSn and HoAuSn and make an angle of 30° in NdAuSn. ErAuSn is cubic (space group $F\bar{4}3m$). At $T = 1.6$ K only a broad peak corresponding to short-range ordering is observed. The observed Néel points range from 2.8 K in PrAuSn to 24 K in GdAuSn. In all title compounds the magnitudes of ordered magnetic moments at 1.6 K derived from neutron diffraction experiments are smaller than the respective free R^{3+} ion values, indicating a strong effect of the crystalline electric field.

1. Introduction

Lanthanide ternary stannides with the composition RTSn, where T is Cu, Ag and Au were reported to have two possible crystal structure types. X-ray powder diffraction measurements indicate that the RTSn phases exhibit the hexagonal, $CaIn_2$ type of crystal structure with random distribution of T and Sn atoms [1–4]. On the other hand, powder neutron diffraction data, which are more sensitive to the differences in neutron scattering lengths of respective nuclei of component elements, favour the occurrence of the hexagonal, LiGaGe type of crystal structure with T and Sn atoms localized in separate lattice sites [5–7], (see section 3.1). The results of a single-crystal neutron diffraction study performed on DyCuSn [8] confirm the presence of the ordered LiGaGe-type structure in this compound.

The information on the magnetic properties of RAuSn compounds has been up to now limited to CeAuSn (antiferromagnetic, $T_N = 4$ K [9]) and GdAuSn (also antiferromagnetic, $T_N = 35$ K [10]). The Mössbauer effect measurements on ^{155}Gd and ^{119}Sn performed for the latter compound suggest the presence of a long-range magnetic order at low temperatures [11].

* Dedicated to Professor Henryk Szymczak on the occasion of his 60th birthday.

+ Corresponding author. E-mail address: szytula@if.uj.edu.pl

0953-8984/97/429053+11$19.50

Continuing our interest in the magnetic properties of RTSn phases [6, 7] we report in this paper the results obtained in the course of magnetometric and neutron diffraction experiments performed for RAuSn compounds.

2. Experimental details

Polycrystalline samples of all title compounds were obtained by arc melting under purified argon atmosphere. High-purity constituent elements were taken in the stoichiometric ratio 1:1:1. The samples, contained in evacuated silica tubes, were annealed at 800 °C for 4 d. X-ray powder data (Cu Kα radiation) were collected at room temperature. They show that all the samples contain a small amount (estimated to be ∼3%) of an unidentified foreign phase. The determined lattice parameters were found to agree well with the data reported in [4] (see table 1).

Table 1. Crystal data for RAuSn compounds.

	Pr $T = 3.6$ K	Nd $T = 15$ K	Tb $T = 17$ K	Dy $T = 10$ K	Ho $T = 11$ K	Er $T = 3.6$ K
a (Å)	4.7199(9)	4.7115(16)	4.6556(17)	4.6448(15)	4.6260(17)	6.6141(29)
c (Å)	7.6192(18)	7.5737(33)	7.4027(34)	7.3782(27)	7.3429(34)	
c/a	1.6143	1.6075	1.5901	1.5885	1.5873	
LiGeGa type						
z_2	0.0593(37)	0.0752(24)	0.0641(35)	0.0652(25)	0.0794(29)	
z_3	0.4730(36)	0.4770(23)	0.4702(34)	0.4833(39)	0.4767(28)	
R_{prof} (%)	6.14	4.38	4.97	4.87	5.75	7.81
R_{Bragg} (%)	2.65	8.19	6.51	9.63	1.54	6.48
$CaIn_2$ type						
z	0.0437(5)	0.0493(8)	0.0474(8)	0.0456(15)	0.0517(10)	
R_{prof} (%)	6.30	4.64	5.04	5.15	8.59	
R_{Bragg} (%)	3.84	10.2	7.34	10.5	1.34	

Magnetic susceptibility measurements have been performed on the polycrystalline samples of RAuSn compounds.

Magnetic susceptibility measurements were carried out in the temperature range from 2 to 300 K using a Cryogenics S100 SQUID susceptometer in the external magnetic fields up to 150 Oe. Additional magnetization data were obtained at 4.2 K in the presence of magnetic fields up to 12 T using a vibrating sample Oxford Instruments VSM 12 T magnetometer. In the determination of the values of the magnetization no demagnetizing corrections have been made.

Neutron diffractograms were obtained on the E6 instrument installed at the BERII reactor in the Hahn–Meitner Institute, Berlin. The incident neutron wavelength was 2.382(3) Å. About 7 g of each sample in a cylindrical vanadium container was taken for data collection. Diffractograms were recorded at a number of temperatures between 1.6 and 40 K. A Rietveld-type program FULLPROF [12] was used to process experimental data. Neutron scattering lengths were adopted following [13]; the form factors for the respective lanthanide ions were taken following [14].

3. Results

3.1. Crystal structure

Neutron diffraction peaks observed at the temperatures above the respective Néel points (see figure 1) were easily indexed on a hexagonal unit cell in the case of RAuSn with R = Pr, Nd, Gd, Tb, Dy and Ho and a cubic structure in the case of ErAuSn.

Two types of crystal structure for RAuSn compounds have been usually considered:

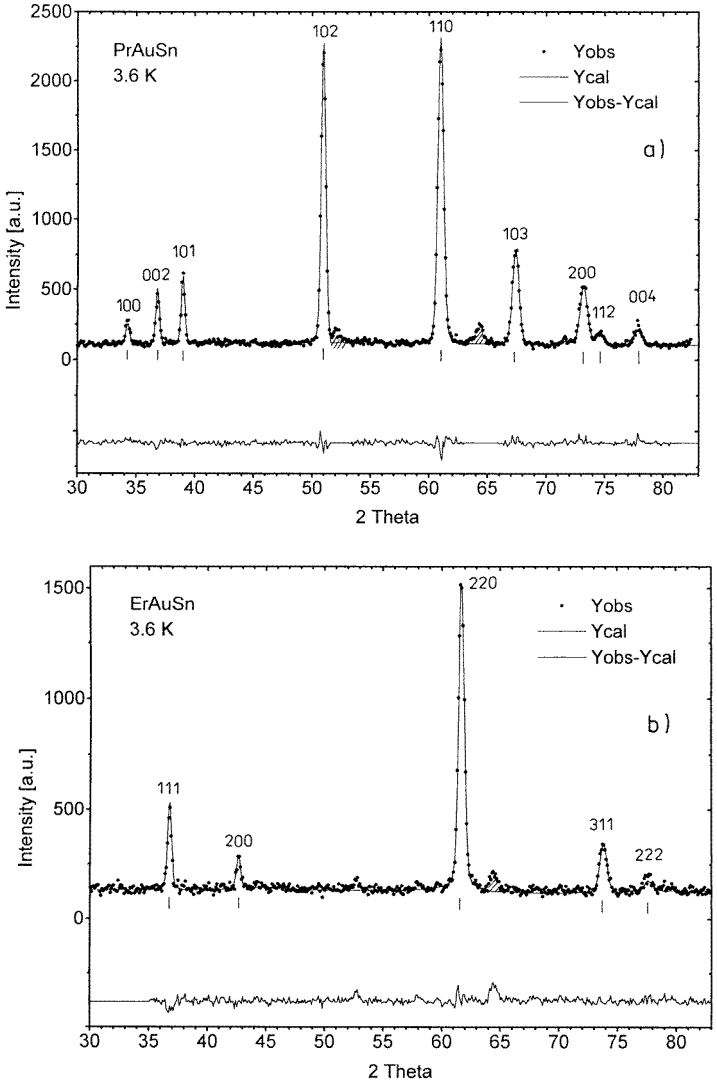

Figure 1. Plots of the observed and calculated neutron diffraction patterns of (a) PrAuSn and (b) ErAuSn at 3.6 K. The open squares represent the observed points and the solid lines the calculated profile and the difference between observed and calculated data (below). The ticks indicate Bragg peaks. The shaded peaks arise from an impurity phase.

(i) $CaIn_2$ type, space group $P6_3/mmc$ with

2R atoms in 2(b) site $0, 0, \frac{1}{4}$ $0, 0, \frac{3}{4}$

2Au and 2Sn atoms at random in the 4(f) site $\frac{1}{3}, \frac{2}{3}, z$ $\frac{2}{3}, \frac{1}{3}, \bar{z}$
$\frac{2}{3}, \frac{1}{3}, \frac{1}{2} + z$ $\frac{1}{3}, \frac{2}{3}, \frac{1}{2} - z$

or

(ii) LiGaGe type, space group $P6_3mc$ with

2R atoms in 2(a) $0, 0, z_1$ $0, 0, \frac{1}{2} + z_1$

2Au atoms in 2(b) $\frac{1}{3}, \frac{2}{3}, z_2$ $\frac{2}{3}, \frac{1}{3}, \frac{1}{2} + z_2$

2Sn atoms in 2(b) $\frac{1}{3}, \frac{2}{3}, z_3$ $\frac{2}{3}, \frac{1}{3}, \frac{1}{2} + z_3$.

The z_1 parameter was fixed at $z_1 = \frac{1}{4}$ to define the origin.

A distinct difference in neutron scattering length values for gold and tin nuclei ($\Delta b = 1.405$ fm) permitted to make a distinction between the above structure types. Two 'agreement' factors were used:

$$R_{prof} = 100 \sum |y_{i\ obs} - y_{i\ calc}| \Big/ \sum y_{i\ obs}.$$

Here, $y_{i\ obs}$ and $y_{i\ calc}$ are the number of counts observed in the position of the Bragg angle after subtraction of the background and calculated by the Rietveld procedure.

$$R_{Bragg} = 100 \sum |I_{obs} - I_{calc}| \Big/ \sum I_{obs}.$$

I_{obs} and I_{calc} are the observed and calculated integrated intensities of Bragg peaks respectively. The values of both factors listed in table 1 favour clearly the ordered LiGaGe-type structure. The neutron diffraction results for ErAuSn (see figure 1(b)) confirm its cubic crystal structure belonging to the cubic system-space group $F\bar{4}3m$ with atoms at the following sites:

4Er in 4(c) $\frac{1}{4}, \frac{1}{4}, \frac{1}{4}$ etc

4Au in 4(a) $0, 0, 0$ etc

4Sn in 4(d) $\frac{3}{4}, \frac{3}{4}, \frac{3}{4}$ etc.

3.2. Magnetic properties

Figure 2 shows the temperature dependence of the reciprocal magnetic susceptibility curves recorded in an external field of 100 Oe for all title compounds. These dependences obey the Curie–Weiss law above 50 K. The numerical fit to the experimental data yielded negative values of paramagnetic Curie temperatures and effective magnetic moment values μ_{eff} close to the free-ion R^{3+} values (see table 2).

The insets show the magnetic susceptibility at low temperatures. These dependences indicate the maximum typical for the change of magnetic structure from an antiferromagnetic to paramagnetic phase for the RAuSn compounds (R = Pr, Gd–Ho). For PrAuGe below

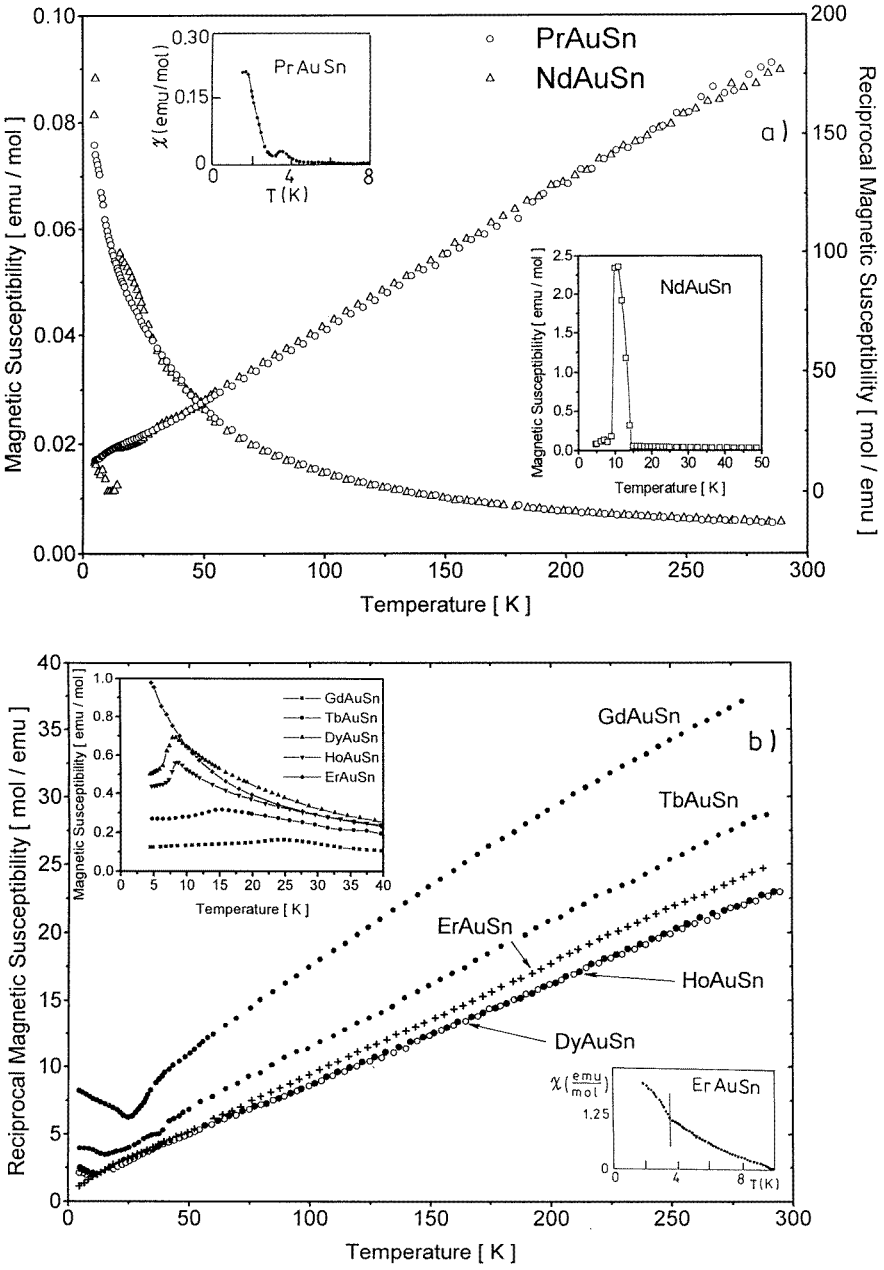

Figure 2. Reciprocal magnetic susceptibility (measured in the external field $H = 10$ Oe)–temperature curves for RAuSn compounds: (a) R = Pr, Nd and (b) R = Gd–Er. The inset shows magnetic susceptibility versus T at low temperatures.

$T_N = 3.5$ K a strong increase of the magnetic susceptibility is observed. The jump of the curve recorded for NdAuSn indicates that a transition from antiferromagnetism to ferromagnetism takes place at 10 K and the Curie point is at 14 K. ErAuSn exhibits a small contribution of magnetization below 3.5 K.

Table 2. Magnetic data for RAuSn compounds.

Compound	T_N (K)		T_C (K)	T_t (K)	θ_p (K)	μ_{eff} (μ_B)		μ (μ_B)			H_{cr} (kOe)
								Exp			
	M[a]	ND				Exp	Theor	M[b]	ND	Theor	
PrAuSn	3.5	2.8			−7.1	3.59	3.58	1.2	0.64	3.12	
NdAuSn		11	14	10	−11.6	3.61	3.62	0.9	1.96	3.27	20
GdAuSn	25	—			−46.7	8.42	7.94	2.45		7	
TbAuSn	15	15			−21.4	9.31	9.72	3.5	5.37	9	
DyAuSn	8	—			−10.2	10.33	10.65	7.0	3.55	10	
HoAuSn	9	9			−14.3	10.35	10.61	7.3	6.38	10	10.35
ErAuSn					−11.1	9.83	9.85	—		9	

M[a], SQUID measurement results.
ND, neutron diffraction experiment.
M[b], magnetic measurements at $T = 4.2$ K and $H = 120$ kOe.

Figure 3 displays the magnetization curves recorded at 4.2 K in the external field up to 120 kOe. They smoothly rise as a function of the external magnetic field for RAuSn with R = Pr, Gd, Tb and Dy. For NdAuSn and HoAuSn the curves at $T = 4.2$ K point to the presence of metamagnetic transitions induced by the external magnetic field.

The magnetization curves for NdAuSn measured at $T = 9$ and 11 K have the different character to those observed at $T = 4.2$ K (see figure 3(b)).

The magnitudes of magnetic moments determined at 4.2 K and $H = 120$ kOe are smaller than the free-ion values for R^{3+} (see table 2). These data indicate that saturation has not been reached at 120 kOe.

3.3. Magnetic structures

Neutron diffractograms recorded at 1.6 K for all title compounds reveal the presence of peaks of magnetic origin (figure 4). With the exception of ErAuSn, they were indexed assuming a magnetic structure characterized by the wavevector $\boldsymbol{k} = |\frac{1}{2}, 0, 0|$ in an orthorhombic unit cell which is related to the hexagonal crystallographic cell by the following relation:

$$a_o = \sqrt{3}a_h \qquad b_o = a_h \qquad c_o = c_h.$$

The suffices o and h refer to the orthorhombic and hexagonal cells respectively.

In the orthorhombic unit cell the magnetic moments localized on lanthanide ions occupy the sites with the following coordinates:

$$S_1(0, 0, \tfrac{1}{4}) \qquad S_2(0, 0, \tfrac{3}{4}) \qquad S_3(\tfrac{1}{2}, \tfrac{1}{2}, \tfrac{1}{4}) \qquad S_4(\tfrac{1}{2}, \tfrac{1}{2}, \tfrac{3}{4}).$$

Group theory [15] considerations point to three possible antiferromagnetic ordering schemes:

$$A = S_1 + S_2 - S_3 - S_4$$
$$C = S_1 - S_2 + S_3 - S_4$$
$$G = S_1 - S_2 - S_3 + S_4.$$

The best agreement with the experimental intensities has been obtained for a collinear antiferromagnetic structure corresponding to the A mode with the magnetic moment parallel to the c-axis in PrAuSn and HoAuSn, making an angle with the c-axis in NdAuSn and

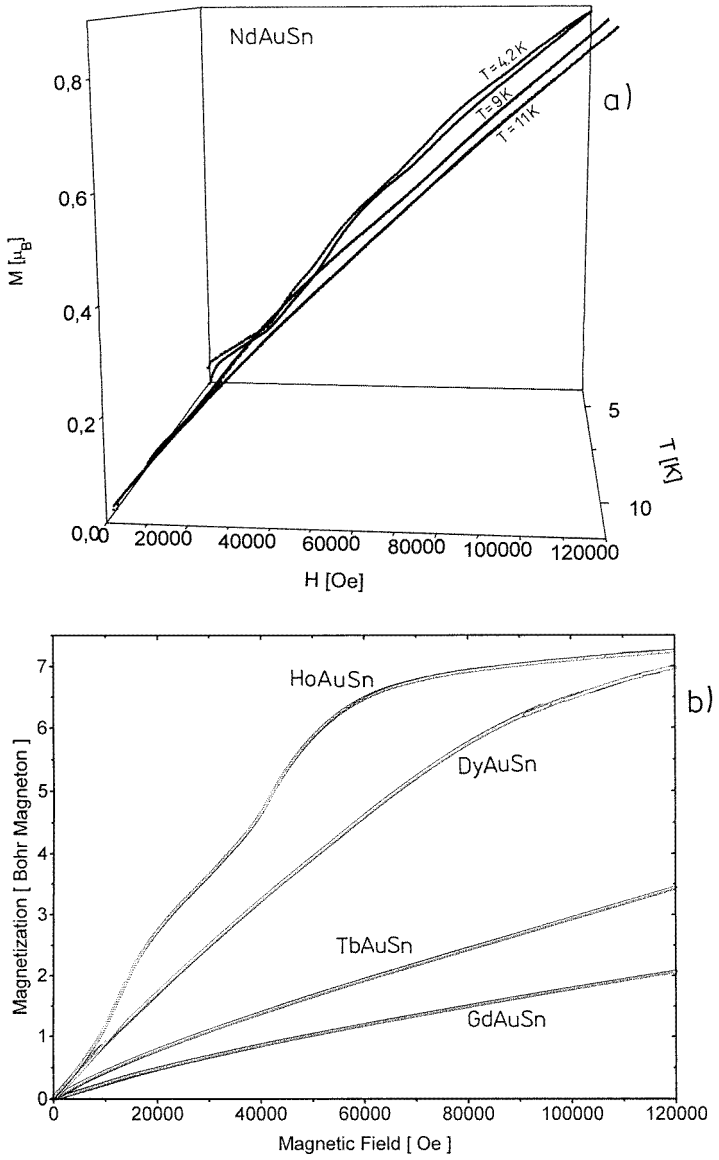

Figure 3. RAuSn: magnetization—magnetic field strength functions recorded for (a) R = Nd at $T = 4.2$, 9 and 11 K and (b) R = Gd–Ho at $T = 4.2$ K.

normal to it in TbAuSn and DyAuSn (see table 3). Neutron diffractograms of NdAuSn recorded at a number of temperatures indicate that the peaks due to antiferromagnetic order vanish at 11 K (see figure 6) but the nuclear peaks above this temperature contain a very small, if any, ferromagnetic contribution. Only one, broad and small in intensity, magnetic peak has been observed on the diffractogram of ErAuSn taken at 1.6 K. Although this peak can be indexed as M(111) in a magnetic unit cell doubled in three directions with respect to the crystallographic cell, it was not possible to establish the magnetic structure of ErAuSn.

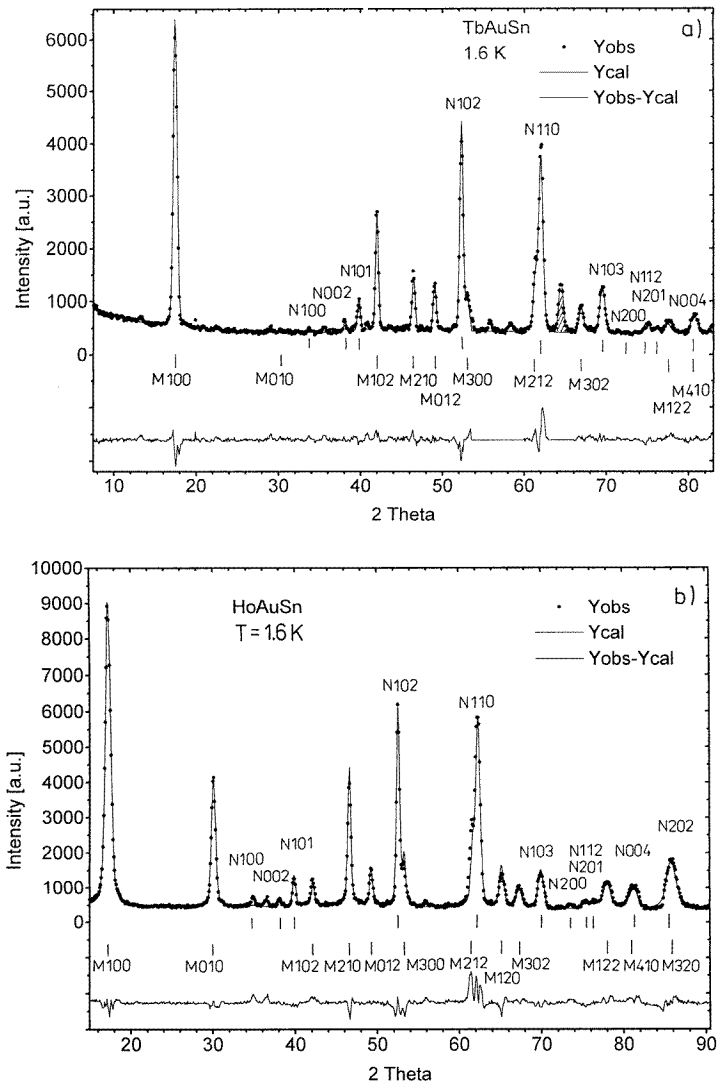

Figure 4. Neutron diffraction patterns calculated and observed at 1.6 K for (a) TbAuSn and (b) HoAuSn. The open squares represent the observed points and the solid lines the calculated profile and the difference between observed and calculated data (below). The upper row corresponds to the reflections related to the crystal structure of the hexagonal LiGaGe type. The lower row corresponds to the magnetic structure described in the orthorhombic unit cell. The shaded peaks arise from RAuSn impurity.

The temperature variation of the strongest magnetic peaks' intensities illustrated in figure 5 gives the Néel points, which are in fair agreement with the data derived from magnetization experiments (table 2). Magnetic structure data are collected in table 3. The observed and calculated neutron intensities and diffractograms recorded at different temperatures between 1.6 and 40 K can be obtained on request from the corresponding author.

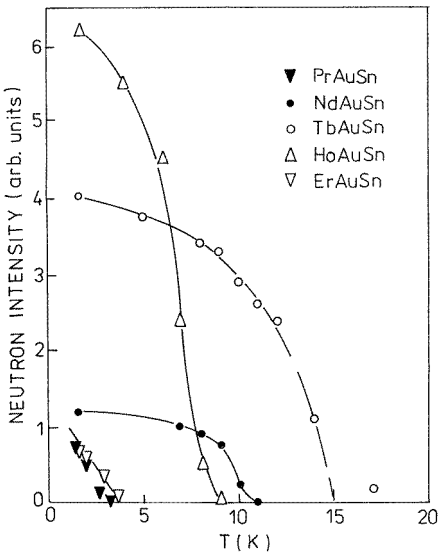

Figure 5. RAuSn: the heights of the most intense magnetic peaks plotted against the temperature.

Table 3. Magnetic structure parameters at 1.6 K for RAuSn compounds.

R	T/T_N	Propagation vector	μ (μ_B)	φ^a (°)	θ^b (°)	R_m (%)
Pr	0.57	$\frac{1}{2}00$	0.64(4)	0	0	13.0
Nd	0.11	$\frac{1}{2}00$	1.96(6)	0	30	18.9
Tb	0.11	$\frac{1}{2}00$	5.37(14)	90	90	8.4
Dy	0.2	$\frac{1}{2}00$	3.55(14)	60	90	11.7
Ho	0.18	$\frac{1}{2}00$	6.38(20)	0	0	6.1
Er		$\frac{1}{2}\frac{1}{2}\frac{1}{2}$	—	—	—	—

[a] The angle with the a_o-axis.
[b] The angle with the c_o-axis.

4. Discussion

In all RTSn (T = Cu, Ag, Au) compounds, the R^{3+}–R^{3+} interionic distances are long enough to exclude any direct magnetic coupling schemes. They amount to ~ 3.6 Å $= c/2$ in the direction of the c-axis and ~ 4.5 Å in the basal plane.

The magnetic ordering schemes observed in RAuSn may be considered as due to two competing factors: the exchange interactions and the crystal electric field (CEF) effect.

One may assume, therefore, that the magnetic ordering observed at low temperatures is due to long-range magnetic interactions of the RKKY type. If so, the paramagnetic Curie temperatures θ_p and the Néel or Curie points should be proportional to the de Gennes function $G = (g-1)^2 J(J+1)$ [16]. Figure 6 shows that for RTSn (T = Cu, Ag, Sn) compounds with LiGaGe-type structure, the de Gennes scaling is not obeyed by compounds containing light lanthanides, but the fit is reasonably good for compounds with heavy lanthanide elements. A similar effect has been found in RGa_2 compounds with the hexagonal AlB_2-type crystal structure [17]. In both families, RTSn and RGa_2, the experimental values of θ_p and T_N (T_C) for compounds with light lanthanides are larger

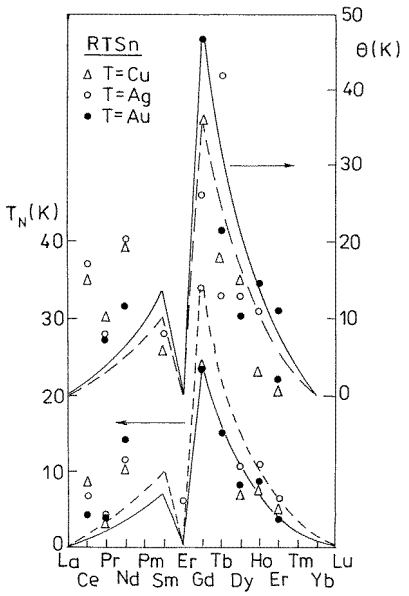

Figure 6. The ordering T_N or T_c and paramagnetic θ_p temperatures of RTSn (T = Cu, Ag, Au) compounds plotted against the number of 4f electrons localized on the R^{3+} ion. The solid and broken lines represent the de Gennes function for RAuSn and RAgSn normalized with respect to GdAuSn and GdAgSn.

than those deduced from the de Gennes model, suggesting the existence of a local coupling between the 4f and conduction electrons which donates a large contribution to the exchange coupling [18].

The second factor which influences the magnetic behaviour of RTSn compounds is the CEF. Its Hamiltonian for hexagonal point symmetry is given by the formula

$$H_{CEF} = B_2^0 O_2^0 + B_4^0 O_4^0 + B_4^3 O_4^3 + B_6^0 O_6^0 + B_6^3 O_6^3 + B_6^6 O_6^6$$

where B_n^m are CEF parameters and O_n^m represent the Stevens equivalents operators. B_2^0 parameters are known only for CeTSn (T = Cu, Ag, Au): they are positive and dominant [19].

This parameter is almost two times larger for CeAuSn as compared to CeCuSn and CeAgSn, thus indicating a large intrinsic contribution of Au atoms to CEF. The ground state moment calculated for CeTSn using CEF wave functions is close to 1 μ_B and is normal to the hexagonal unique axis, in fair agreement with the results of a neutron diffraction experiment carried out for CeAgSn [7].

The magnitudes of the ordered magnetic moment localized on lanthanide ions observed at 1.6 K are much smaller than the free-ion values (see table 2). One may conclude that this is also an effect of the action of the CEF.

Acknowledgments

The kind hospitality and financial support granted by the Hahn–Meitner Institute to perform neutron experiments is gratefully acknowledged by two of the authors (SB and JL).

This work has been supported by the European Community (PECO program) and the State Committee for Scientific Research in Poland with grant No 2P03B 08708.

References

[1] Szytuła A and Leciejewicz J 1994 *Handbook of Crystal Structures and Magnetic Properties of Rare Earth Intermetallics* (Boca Raton, FL: Chemical Rubber Company)

[2] Dwight A E 1976 *Proc. 12th Rare Earth Research Conf.* ed C E Lundin (Denver, CO: Denver Research Institute) p 480

[3] Mazzone D, Rossi D, Marazza R and Ferro R 1981 *J. Less-Common Met.* **80** 47

[4] Komerovskaya L P, Skolozolva R V and Filetova I V 1983 *Dopov. Akad. Nauk Ukr. RSR Ser. A* **45** 82

[5] Baran S, Leciejewicz J, Stüsser N, Szytuła A and Tomkowicz Z 1997 *Solid State Commun.* **101** 631

[6] Baran S, Ivanov V, Leciejewicz J, Stüsser N, Szytuła A, Zygmunt A and Ding Y 1997 *J. Alloys Compounds* at press

[7] Baran S, Leciejewicz J J, Stüsser N, Szytuła A, Zygmunt A and Ding Y 1997 *J. Magn. Magn. Mater.* **170** 143

[8] Pöttgen R and Kotzba G 1996 *J. Alloys Compounds* **245** L9

[9] Lenkewitz M, Corsépius S and Stewart G R 1996 *J. Alloys Compounds* **241** 121

[10] Oesterriecher H 1977 *J. Less-Common Met.* **55** 131

[11] Bialić D, Kruk R, Kmieć R and Tomala K 1997 *J. Alloys Compounds* at press

[12] Rodriguez-Carvajal J 1993 *Physica* B **192** 55

[13] Sears V F 1992 *Neutron News* **3** 26

[14] Freeman A J and Desclaux J P 1979 *J. Magn. Magn. Mater.* **12** 11

[15] Bertaut E F 1968 *Acta Crystallogr.* A **24** 217

[16] de Gennes P G 1962 *J. Physique Radium* **23** 510, 630
de Gennes P G 1962 *J. Physique Radium* **23** 630

[17] Ball A R, Gignoux D, Schmitt D and Zhang F Y 1995 *J. Magn. Magn. Mater.* **140–4** 1121

[18] Belorizky E, Niez J J and Levy P M 1981 *Phys. Rev.* B **23** 3360

[19] Adroja D T, Rainford B D and Neville A J 1997 *J. Phys.: Condens. Matter* **9** L391